Tunable SERS in Gold Nanorod Dimers through Strain Control on an Elastomeric Substrate

Kristen D. Alexander,*,[†] Kwan Skinner,[†] Shunping Zhang,[‡] Hong Wei,[‡] and Rene Lopez[†]

[†]Department of Physics and Astronomy, University of North Carolina, Chapel Hill, North Carolina 27599, United States, and [‡]Beijing National Laboratory for Condensed Matter Physics, Institute of Physics, Chinese Academy of Sciences, Beijing 100190, China

ABSTRACT In this Letter we provide experimental verification of the interparticle distance dependence of the SERS enhancement factor in 1 μm gold gapped nanorods. Au dimers are fabricated from electrochemically grown heterogeneous Au–Ag–Au nanorods and deposited on a stretchable elastomer film which allows active and reversible tuning of the interparticle gap on the sub-5-nm level. Significantly, this technique allows the distance dependence to be tracked using a single dimer, thereby avoiding enhancement factor reproducibility issues arising from morphological differences in disparate nanoparticle pairs.

KEYWORDS Nanorod, SERS, electrodeposition, elastomer, interparticle gap, AAO template

The integration of surface-enhanced Raman spectroscopy (SERS) into various chemical sensing technologies is a matter of increasing scientific as well as societal interest. In particular, applications of SERS to chemical sensors with the ability to detect substances on the single molecule level[1−3] stand to benefit a broad range of fields and are currently receiving a great deal of attention from researchers. However, the development of such technologies necessitates a thorough understanding of the mechanisms from which SERS arises and a great deal of progress has been made, especially on the theoretical front, since its discovery in 1977.[4] Unfortunately, the development of experiments to test these theories has been severely hampered by enhancement factor reproducibility issues. This rings especially true with regard to the detection at the single molecule level because detectable signals arise from a small number of plasmonically coupled nanostructures rather than being averaged over an entire substrate, making it extremely sensitive to small chemical and morphological differences that invariably exist between disparate nanostructures.

Noble metal nanoparticles have long been recognized for their unique plasmonic properties, particularly their ability to couple to each other through near field interactions, giving rise to a variety of interesting surface enhanced phenomena. Particle–particle plasmonic coupling is particularly sensitive to subtle changes in geometry, arising from variances in nanoparticle size,[5] shape,[6] crystal face,[7] surface roughness,[8] and particle–particle spacing.[9−14] This presents the possibility of making SERS substrates that are infinitely tunable, provided the techniques for fabricating the desired structures

are available. The nanoparticle dimer has emerged as one of the most efficient and widely used configurations in studies involving surface-enhanced phenomena, producing intense electromagnetic fields in the interstices of a reasonably simple structure. Theoretical studies have shown that variations in particle–particle spacing have a particularly strong effect on the strength of these "gap plasmons" between highly resonant (<100 nm) particles, with changes in the spacing as small as 1 nm causing the SERS signal to rise or fall by amounts as large as an order of magnitude.[15,16] For larger particles this effect is less dramatic[17] but nevertheless, the distance dependence of the SERS enhancement has been limited by experimental variation of multiple parameters. In past experiments, researchers have examined collections of seemingly identical particle pairs with nominally controlled spacings,[9,11,13,18,19] but which surely possess large variations in the crucial parameters listed above. Even Raman active molecule coverage cannot be warranted to be identical, thus geometrically similar clusters often present very different SERS effects. While there has been some success producing reliable surface-averaged enhancement factors over large areas,[20,21] the ability to probe specific parametric dependences of the SERS effect itself is inextricably dependent on the ability to make repeated measurements on truly identical individual nanostructures. Therefore, a technique that provides the ability to vary a single parameter (e.g., particle–particle spacing) while holding all the other morphological aspects constant is both desirable and necessary.

In this Letter, we report on a simple method by which the spacing between two adjacent nanorods can be changed by varying the strain applied to an elastomeric silicone rubber substrate. The deposition of nanorod dimers on a

---

stretchable substrate permits the coupling of macroscopic changes in substrate length to nanometer-sized movements between particles, resulting in a tunable interparticle gap size. Applying this technique, we have verified the interparticle distance dependence of the SERS enhancement of individual pairs of gold nanorods, the first time that such a feat has been realized. This technique provides several significant benefits: (a) the controlled strain provides access to small interparticle spacings that would otherwise be impossible to achieve with current lithographic methods, (b) particle separation can be optimized, thereby creating maximum SERS signal strength, and (c) the process is completely reversible and repeatable for a given set of dimers. Additionally, this technique relies on basic wet chemical processing techniques and can be easily adapted to a wide range of particle sizes, shapes, and compositions, providing a promising alternative for studies involving the precise placement of nanoparticle structures.

Recently, there has been a great deal of interest in extending spectroscopic capabilities to nanogap structures with larger segment lengths. Larger structures provide the option of being addressed electrically and can more easily be identified and tracked using optical microscopy, an important factor in our approach. In contrast to their smaller counterparts, nanostructures several hundred nanometers in length support multipolar resonances[22] that are periodic in nature, providing large enhancements at specific lengths and producing almost no signal at others for a given excitation source frequency.[19,23] For these experiments, we chose nanorod segments 1 μm in length which were expected to present resonant behavior when illuminated with a 785 nm source according to the relation[8]

$$L = \frac{n - \frac{1}{2}}{2}\lambda \qquad (1)$$

where L, λ, and n are the segment length, the surface plasmon polariton wavelength, and the order of the multipole, respectively.

In order to determine the gap dependence of the enhancement factor at the interparticle junction, we performed full-wave electromagnetic calculations based on the finite element method (FEM, COMSOL Multiphysics). The rod dimer configuration simulated in this study consisted of two cylindrical segments ranging from 200 to 320 nm in diameter and 1 μm in length, consistent with the size of the nanorods produced in this experiment. Incident plane wave radiation impinged normally on the dimer, with the electric field polarized parallel to the dimer axis. Optical constants of gold ($\varepsilon_{Au} = -23.02 + 1.436i$) at the vacuum wavelength of 785 nm were taken from Johnson and Christy's publication.[24] In order to compare our simulation results with the SERS enhancement factor (EF) obtained experimentally
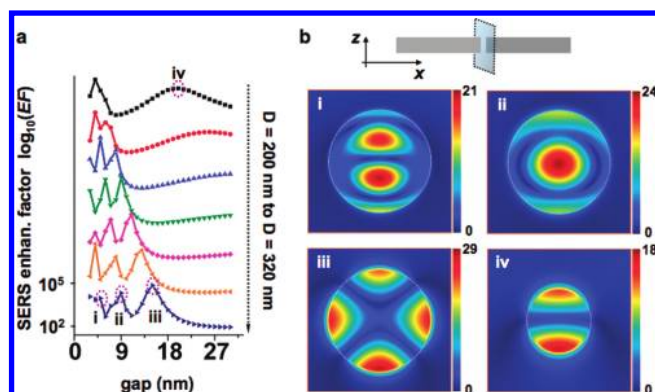

FIGURE 1. (a) FEM calculated surface-averaged SERS enhancement factor (EF) as a function of gap distance for gold rod dimers of different sizes ($D = 200$ nm to $D = 320$ nm from top to bottom in increments of 20 nm). (b) Calculated $|E_x|$ distribution in the vertical plane at the center of the gap (indicated in the inset) for modes i to iv.

from an adsorbed monolayer, we estimated the surface averaged SERS EF using the relation[25]

$$EF = \frac{\int g \, dS}{\int dS} \qquad (2)$$

where

$$g = \frac{|E_{pump}|^2 |E_{Stokes}|^2}{|E_0|^4}$$

denotes the localized SERS EF and E_0, E_{Stokes}, and E_{pump} are the incident, enhanced Raman, and enhanced incident electric fields, respectively and the integral was taken over a cross-section in the gap region 1 nm away from the metal surface. Because the absorption peaks for these rods are broad and the wavelengths of the enhanced excitation and Raman radiation are close enough to fall under the umbrella of this peak, we use the approximation $|E_{pump}|^2 |E_{Stokes}|^2 \approx |E_{pump}|^4$ (see Supporting Information). The SERS enhancement factor (EF) was evaluated at a distance of 1 nm from the metal surface to avoid breakdown of the classical approach and numerical instabilities at the particle surface as well as to coincide with the distance at which an adsorbed reporter molecule (benzenethiol was used in this study) would likely be located.

The calculated relations between the SERS EF and particle–particle spacing for gold rod pairs 200–320 nm in diameter are shown in Figure 1a. The results of these simulations reveal optimal gap sizes for these particular rod pairs below approximately 20 nm, indicating the target range for the experimental particle–particle separation studies. Within this range, the dimer is expected to create a surface averaged SERS EF on the order of 10[5] when excited at its resonance frequency. Here we also note that multiple maxima appear at these small interparticle distances, arising
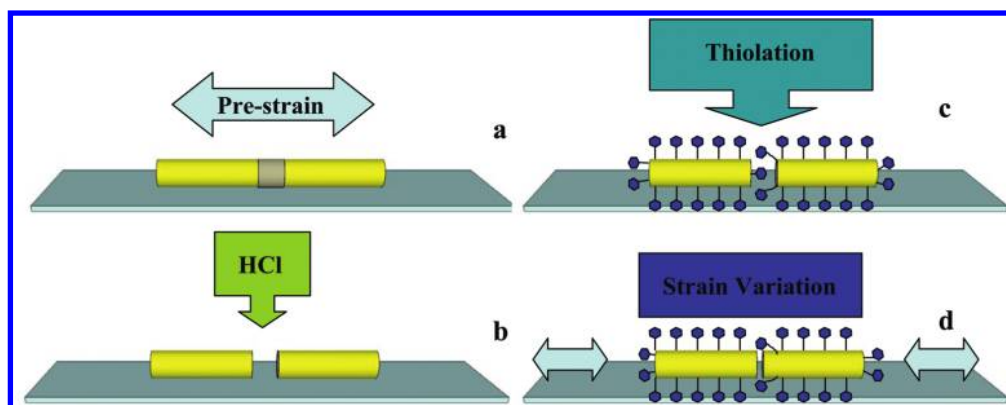
FIGURE 2. A schematic illustration of the dimer fabrication process. (a) Heterogenenous nanorods are deposited on a prestrained silicone rubber film. (b) An aqueous solution of hydrochloric acid is used to etch away the silver spacer layer. (c) The entire substrate is immersed in a 1 mM ethanolic solution of thiophenol to functionalize the dimer. (d) Substrate strain is varied to move the nanorod segments relative to each other.

from the plasmon resonances of the gold dimer. As the diameter of the nanorod segment increases, these resonances tend to shift to larger gap separations. Large local electric fields are generated by the electric field enhancements in the gap, which will serve to enhance the Raman excitation of the reporter molecule. The distributions of the E_x component of the local electric field for different resonance peaks are shown in Figure 1b, each corresponding to one peak in the EF−distance relation shown in Figure 1a. The rod diameters in (i−iii) are 320 and 200 nm in (vi). The gap distances are 5, 9, 15, and 20 nm in (i−vi), respectively. It should be noted that in order to evaluate these resonances for SERS enhancement, the integral over the absorbing surface is critical due to the spatial distribution of the enhanced electric fields. This differs from calculations involving small nanoparticle dimers where the EF from a single position (e.g., the center of the gap) gives a result similar to the surface averaged enhancement factor.

To experimentally realize the dimer configuration described above, we have fabricated nanorod dimers using a modified version of on-wire lithography (OWL).[26] Nanorod dimers were created using a combination of electrodeposition and wet chemical etching. Au−Ag−Au nanorods were grown via DC electrochemical deposition in 200 nm diameter anodic alumina oxide (AAO) templates (Whatman). For this experiment, two Au cylinders (1 μm in length) were separated by a Ag segment (∼80 nm in length) designed to serve as a sacrificial spacer layer. Immediately following the electroplating, the templates were placed in a 3 M NaOH solution for 60 min to dissolve the alumina and, afterward, were washed in ethanol and suspended in a 20:80 mixture of ethanol and water to prevent aggregation. A typical nanorod dimer pair is shown in the inset of Figure 4. SEM imaging provided information about the dimensions of the nanorods constituting a typical dimer pair. The diameters of the resulting nanorods are defined by the pores in the host AAO template (nominal values ranging from 200 to 320 nm). Nanorods were then dropcast on a prestrained silicone

rubber film and blown dry with N_2 (Figure 2a). The use of heterogeneous nanorods as a precursory structure provides several technical advantages over randomly deposited nanostructures previously used in SERS experiments.[2,18,27] One of the most significant advantages is customizable gap sizes designed into the resulting nanorod dimer pair after etching of the sacrificial layer. Other researchers used an oxide backbone to fix the particle interspacing.[19] However, in our approach this distance is not critical and in fact it just needs to be in the desired range since it will be tuned via the elastomeric substrate. Next, the film was immersed in a 6 M aqueous solution of HCl and water for 10 min at room temperature to etch away the Ag spacer (Figure 2b). The substrate was then removed from the HCl solution and rinsed in deionized water for 2 min to remove excess HCl. Finally, the completed dimers were immersed in a 1 mM ethanolic solution of benzenethiol (BT) for 24 h at room temperature to ensure thorough functionalization of the nanorods with the reporter molecule (Figure 2c).

Control of the interparticle gap was achieved by modulating the strain of the elastomer substrate using a hysteresis-free translation stage outfitted with a fine micrometer (Figure 2d). Strain measurements at the macro- and microscopic levels are known to be linearly proportional and we verified this for the specific case of our samples by observing changes in separation between nanoparticle pairs in response to substrate deformation. This test was extended to the 300 nm particle−particle length scale, the smallest distances that can reliably be measured with a confocal microscope. Preliminary stretching experiments on 1 μm polystyrene beads deposited on the elastomer reveal a linear relationship between the strain measured at both the macroscopic (i.e., total change in length of the elastomer film) and the microscopic (i.e., change in distance between individual nanoparticles determined through confocal imaging) levels which is presumed to extend down to the molecular scale (see Supporting Information).

Unlike isotropic pointlike nanoparticles which should, under ideal conditions, only be in contact with the substrate at a single point, the elongated nanorod geometry necessitates the calculation of customized strain−distance scaling factors for each dimer pair. The elongated shaft of the nanorod provides a large area that can potentially be in contact with the substrate when the nanorod is initially deposited on the substrate. When the elastomer is deformed, the rigid nanorod resists deformation and subsequently detaches from the substrate at all but a single point. The distance between these two points of attachment for each dimer pair determines the linear scaling factor that governs the relationship between the strain applied to the substrate and the actual distance the nanorods move relative to each other. For instance, if two ideal 1 μm cylindrical nanorods aligned end-to-end were both connected to the substrate at the center of their long axes, then the distance between these points of attachment for touching rods would be exactly 1 μm. To open a 5 nm gap between the rods, the distance between these two points would need to be increased to 1005 nm, necessitating a 0.5% strain applied to the substrate. If the length of the elastomeric substrate is 1 cm, this length would need to be increased by 50 μm, a movement that is easily achieved with a micrometer stage. Likewise, to open a clearly visible gap, say 500 nm, the substrate would need to be stretched to 1.5 cm in length, highlighting the necessity of a substrate material with sufficient recoverable strain.

To obtain the customized scaling factors used in these experiments, unetched nanorods were deposited on an elastomeric substrate under sufficient strain to bring individual segments into head-to-head contact upon etching and relaxation of the film. Next, the substrate was immersed in a 6 M aqueous solution of HCl for approximately 10 min to dissolve the silver spacer layer and substrate strain was subsequently reduced to bring the particles into physical contact. The substrate was then strained again to create a large (approximately 1000 nm) gap between the nanorods which could be measured optically. This measured distance was then correlated with the change in length of the substrate (measured with the stage micrometer) from which the nanoscopic movements between the particles could be deduced. Here, it is important to emphasize that because the distance between the points of contact to the substrate is different for every nanorod pair, it was necessary to perform this correlation for every dimer used in this study.

SERS signal measurements from individual dimers were obtained using a Leica microscope equipped with a confocal Raman spectroscopic system (Renishaw, inVia) with a 45 mW 785 nm laser excitation source. All spectra were measured using a 50× objective with a numerical aperture of 0.75. The Raman signal was collected by a TE air-cooled 576 × 400 CCD array preceded by two notch filters (OD > 12) to block the laser line. The dimers were illuminated by centering the laser spot (diameter ∼2 μm) over the central gap, and spectra were subsequently collected with an integration time of 60 s. Exposure to intense laser radiation can degrade the reporter mol-
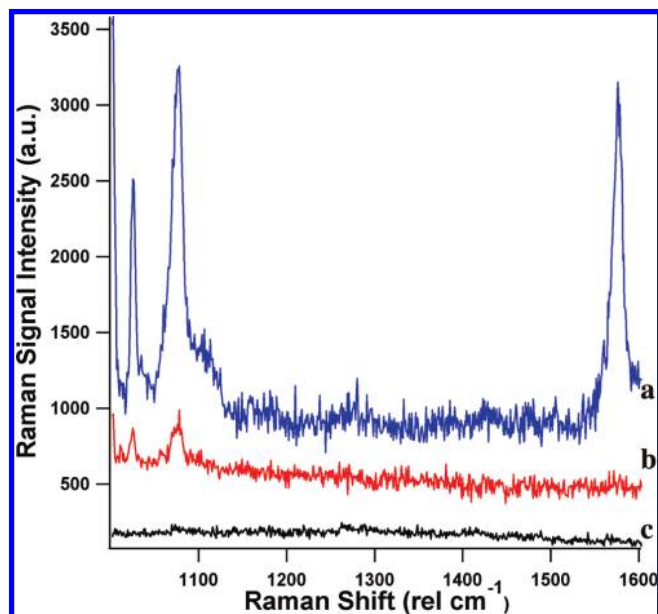

FIGURE 3. (a) A spectrum of a 320 nm diameter nanorod pair functionalized with benzenethiol (approximately 10 nm separation) taken with 785 nm laser light polarized along the dimer axis. (b) A spectrum of the same dimer with light polarized perpendicular to the dimer axis. (c) A spectrum of the same nanorod pair at a separation of 300 nm. Traces are artificially offset for clarity.

ecule over time, so stability tests were performed to determine a laser power that would allow the signal to remain stable. It was determined that 100 μW measured at the sample surface provided a signal that was sufficiently stable and strong. The dependence of the SERS signal strength on the interparticle spacing was tracked by measuring the Raman signal from an individual nanorod pair repeatedly as the substrate strain was varied with the micrometer in small increments. In order to ensure reproducibility of our own results and to further rule out the possibility of our data being skewed by laser-induced degradation of the reporter molecule, all measurements were performed over three stretching cycles for each dimer considered here. The results of a typical spectrum for a particle−particle separation of ∼10 nm are shown in Figure 3. The most pronounced peaks appear at 1000 cm^{-1} (ring out-of-plane deformation and C−H out-of-plane bending), 1080 cm^{-1} (C−C symmetric stretching and C−S stretching), and 1577 cm^{-1} (C−C symmetric stretching).[27]

Normalized data depicting the dependences of the intensity of the Raman band at 1080 cm^{-1} to the dimer gap separation are presented in Figure 4 and are in good agreement with our theoretical predictions. Here, we highlight the fact that because the length, width, and gap roughness of the dimers used in this study were not identical, the data presented in Figure 4 are only representative of a single dimer. However, data taken from two other dimers displayed trends matching the ones shown here and were in general agreement with the results of our FEM simulations in the sense that they showed enhanced Raman signals at gap distances under 20 nm (data shown in Supporting Information). Furthermore, to strengthen the argument that the
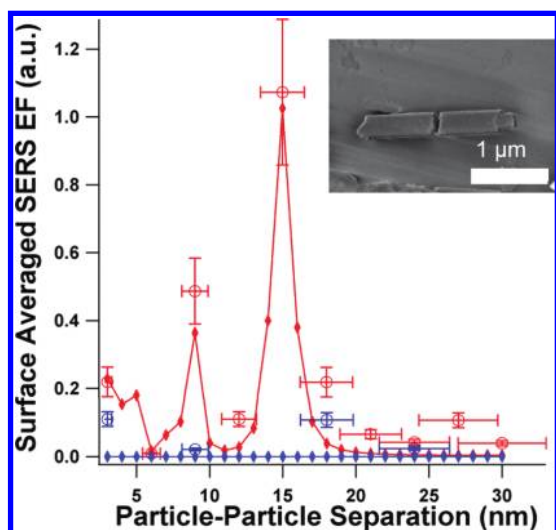
FIGURE 4. Red and blue traces show the calculated values of the surface-averaged SERS enhancement factor for polarization parallel and perpendicular to the dimer axis, respectively. Red circles denote the experimental values for the SERS enhancement factor for parallel-to-axis illumination. Blue circles denote experimental values for perpendicular-to-axis illumination. Inset: A SEM image of a typical nanorod pair used in these experiments. *Y*-error bars calculated from observed dispersion in EF data. *X*-error bars calculated as described previously. Inset: SEM image of a typical nanorod dimer pair.

origin of the strong variation in the Raman enhancement is indeed the dispersion of the dimer modes, we have calculated the extinction spectra for our nanorod dimer pairs. These results illustrate the tight link between the strength of the enhanced Raman signal and the absorption peaks, which strengthens this claim (see Supporting Information). Finally, it is important to note that one of the limiting factors in this experiment was to find SERS-active nanorod pairs that were aligned along the translational stage axis. Optical tracking of individual structures reveals that dimers not aligned along the direction of applied strain tend to move at some angle to, rather than along, the dimer axis when strain is varied. This changes the morphology of the gap and inhibits accurate assessments of changes in interparticle spacing. For this reason, we were careful only to conduct measurements on nanorod pairs aligned directly along the axis of strain.

Gap estimate error was calculated from the diffraction limited measurement of the relative position of the particles as there is a $\lambda/2$ error determining the distance between them. This measurement was made at the maximum separation of 1000 nm between the rods and, assuming that 400 nm light gives the sharpest image, this yields an uncertainty in the relative position of 20% that carries out to all deduced separation values. Significantly, the largest enhancement observed in our experimental measurement occurs at an interparticle separation of approximately 15 nm, in close agreement with the simulated EF. While the small number of measured points in our data set does not exactly reproduce the simulated EF values, it is nonetheless a strong indication that the true position of the peak is in the vicinity

of this particular gap size. This is particularly obvious in the measurements taken from other dimers in this study (see Supporting Information) where the exact height and locations of the peaks are not commensurate with those predicted by FEM. Furthermore, it is also important to note that the dimers in our model are perfect cylinders which do not include surface imperfections, the polycrystalline nature of the segments, or the inherent roughness of the interparticle gap, which would account for the observable SERS signal for perpendicular excitation which was is not predicted by FEM calculations. In a recent study on the structural effects of gap roughness on the SERS enhancement, it was demonstrated that roughened gapped rod pairs exhibited significant resonance broadening from plasmon dephasing that occurs due to protrusions that cause irregularities in interparticle spacing (and, thus, interaction) between segments.[17] As the nanorods used in this study are inherently rough at the interparticle interface, it is very likely that the peak would be smeared across a certain range of interparticle separations.

We have also extended our investigation to include the situation in which the incident electric field is oriented both parallel and perpendicular to the dimer axis. Previous studies have demonstrated that the sensitivity of the SERS signal to the polarization of the incident radiation was most pronounced at small separations (i.e., when the resultant SERS signal is large) and gradually wanes as particle–particle separation is increased.[28,29] This is largely due to the fact that, at larger separation distances, the dipole coupling weakens, leaving higher order resonances which are not necessarily strongly polarization dependent to contribute to the bulk of the measured signal strength. Both our simulation results as well as our experimental findings show a large contrast between polarizations at separations less than 15 nm with this difference becoming smaller at larger interparticle distances, consistent with previous reports.

In conclusion, we have developed a facile method to control SERS-active dimer spacing through the fabrication of nanorod heterostructures on elastomeric substrates. Subsequent measurements of the SERS enhancement factor over a range of interparticle separations yielded a trend consistent with what was predicted by FEM simulations for primary mode resonances. This method improves upon methods proposed in recent publications[30] because the ideal interstitial spacing can effectively be designed into the nanorod growth process, eliminated the need for excessive tuning to bring the dimer into resonance. This is an important advantage for potential scientific and commercial applications of this technique, as it reduces the need for excessive particle movement to produce large SERS enhancement factors. Furthermore, since every heterostructure can be made into a nanorod dimer, this technique provides a high throughput, consistent and tunable means by which SERS-active structures can be created. This technique can be extended to probe more complex structures

NANO _LETTERS_

such as nanoparticle chains and plasmonic coupling between nanoparticles of different materials (experiments in progress).

Supporting Information Available. Experimental procedures, extinction spectrum simulations, and more examples of the EF gap dependence in Au nanorod dimers. This material is available free of charge via the Internet at http://pubs.acs.org.

REFERENCES AND NOTES

(1) Kneipp, K.; Wang, Y.; Kneipp, H.; Perelman, L. T.; Itzkan, I.; Dasari, R.; Feld, M. S. _Phys. Rev. Lett._ **1997**, _78_, 1667–1670.
(2) Nie, S. M.; Emery, S. R. _Science_ **1997**, _275_, 1102–1106.
(3) Xu, H. X.; Bjerneld, E. J.; Kall, M.; Borjesson, L. _Phys. Rev. Lett._ **1999**, _83_, 4357–4360.
(4) Jeanmaire, D. L.; Vanduyne, R. P. _J. Electroanal. Chem._ **1977**, _84_, 1–20.
(5) Krug, J. T.; Wang, G. D.; Emory, S. R.; Nie, S. M. _J. Am. Chem. Soc._ **1999**, _121_, 9208–9214.
(6) Hao, E.; Schatz, G. C. _J. Chem. Phys._ **2004**, _120_, 357–366.
(7) Kambhampati, P.; Child, C. M.; Foster, M. C.; Campion, A. _J. Chem. Phys._ **1998**, _108_, 5013–5026.
(8) Li, S.; Pedano, M. L.; Chang, S.-H.; Mirkin, C. A.; Schatz, G. C. _Nano Lett._ **2010**, _10_, 1722–7.
(9) Su, K. H.; Wei, Q. H.; Zhang, X.; Mock, J. J.; Smith, D. R.; Schultz, S. _Nano Lett._ **2003**, _3_, 1087–1090.
(10) Jiang, J.; Bosnick, K.; Maillard, M.; Brus, L. _J. Phys. Chem. B_ **2003**, _107_, 9964–9972.
(11) Gunnarsson, L.; Bjerneld, E. J.; Xu, H.; Petronis, S.; Kasemo, B.; Kall, M. _Appl. Phys. Lett._ **2001**, _78_, 802–804.
(12) Jain, P. K.; El-Sayed, M. A. _J. Phys. Chem. C_ **2008**, _112_, 4954–4960.
(13) Rechberger, W.; Hohenau, A.; Leitner, A.; Krenn, J. R.; Lamprecht, B.; Aussenegg, F. R. _Opt. Commun._ **2003**, _220_, 137–141.
(14) Xu, H. X.; Aizpurua, J.; Kall, M.; Apell, P. _Phys. Rev. E_ **2000**, _62_, 4318–4324.
(15) Futamata, M.; Maruyama, Y.; Ishikawa, M. _J. Phys. Chem. B_ **2003**, _107_, 7607–7617.
(16) Alexander, K. D.; Hampton, M. J.; Zhang, S. P.; Dhawan, A.; Xu, H. X.; Lopez, R. _J. Raman Spectrosc._ **2009**, _40_, 2171–2175.
(17) Pedano, M. L.; Li, S. Z.; Schatz, G. C.; Mirkin, C. A. _Angew. Chem., Int. Ed._ **2010**, _49_, 78–82.
(18) Moskovits, M.; Jeong, D. H. _Chem. Phys. Lett._ **2004**, _397_, 91–95.
(19) Qin, L. D.; Zou, S. L.; Xue, C.; Atkinson, A.; Schatz, G. C.; Mirkin, C. A. _Proc. Natl. Acad. Sci. U.S.A._ **2006**, _103_, 13300–13303.
(20) Gopinath, A.; Boriskina, S. V.; Premasiri, W. R.; Ziegler, L.; Reinhard, B. M.; Dal Negro, L. _Nano Lett._ **2009**, _9_, 3922–3929.
(21) Lu, J.; Chamberlin, D.; Rider, D. A.; Liu, M. Z.; Manners, I.; Russell, T. P. _Nanotechnology_ **2006**, _17_, 5792–5797.
(22) Wei, H.; Reyes-Coronado, A.; Nordlander, P.; Aizpurua, J.; Xu, H. _ACS Nano_ **2010**, _4_, 2649–2654.
(23) Qin, L.; Banholzer, M. J.; Millstone, J. E.; Mirkin, C. A. _Nano Lett._ **2007**, _7_, 3849–3853.
(24) Johnson, B.; Christy, R. W. _Phys. Rev. B_ **1972**, _6_, 4370–4379.
(25) Novotny, L.; Hecht, B. _Principles of Nano-Optics_; Cambridge University Press: Cambridge, 2006.
(26) Payne, E. K.; Shuford, K. L.; Park, S.; Schatz, G. C.; Mirkin, C. A. _J. Phys. Chem. B_ **2006**, _110_, 2150–2154.
(27) Hu, J. W.; Zhao, B.; Xu, W. Q.; Fan, Y. G.; Li, B.; Ozaki, Y. _Langmuir_ **2002**, _18_, 6839–6844.
(28) Banholzer, M. J.; Li, S. Z.; Ketter, J. B.; Rozkiewicz, D. I.; Schatz, G. C.; Mirkin, C. A. _J. Phys. Chem. C_ **2008**, _112_, 15729–15734.
(29) Sawai, Y.; Takimoto, B.; Nabika, H.; Ajito, K.; Murakoshi, K. _J. Am. Chem. Soc._ **2007**, _129_, 1658–1662.
(30) Huang, F.; Baumberg, J. J. _Nano Lett._ **2010**, _10_, 1787–92.